Function of the MexB Efflux-Transporter Divided into Two Halves†

Shima Eda, Hiroshi Yoneyama, and Taiji Nakae*

Department of Molecular Life Science, Tokai University School of Medicine, 143 Shimokasuya, Isehara, 259-1193, Japan

Received January 7, 2003; Revised Manuscript Received April 28, 2003

ABSTRACT: The MexA-MexB-OprM efflux pump exports structurally and functionally diverse xenobiotics and confers multi-drug resistance on *Pseudomonas aeruginosa* cells. The MexB transporter traverses the inner membrane twelve times, bears two large periplasmic domains and has two homologous tandem repeats. To test whether two homologous halves of MexB function independently or interdependently, the protein was divided medially into two halves, each consisting of six amino- and carboxyl-proximal transmembrane segments. When two halves of MexB were coexpressed from independent open reading frames, the cells lacking chromosomal *mexB* exhibited restored antibiotic resistance at a level close to that in the cells producing a full-length MexB. In contrast, MexB protein containing either an amino- or carboxyl-half fragment failed to transport antibiotics. To test whether the amino- and carboxyl-proximal halves were present in a complex, we purified the histidine-tagged carboxyl-proximal half molecule using nickel-chelate chromatography from the cells that coexpressed two halves. The results showed that the nonhistidine-tagged amino-proximal half was co-purified with the carboxyl-proximal half, thereby indicating that the amino-proximal half fragment was tightly associated with the carboxyl-proximal half molecule. These findings suggest that the presence of both amino- and carboxyl-halves of MexB in a complex is essential for transport activity.

An increasing body of reports on the presence of active xenobiotic efflux transporters in bacteria shows that the efflux system serves as a general mechanism to protect bacteria from potential hazards including antibiotics, synthetic chemotherapeutic agents, surfactants, and heavy metals (*1*, *2*). When chemotherapeutic agents were the substrate of the transporter, the intracellular concentration of the drug decreased resulting in bacterial resistance to the agents (*3*−*5*). This is a major problem in hospitals because a majority of xenobiotic efflux pumps transport structurally and functionally dissimilar chemotherapeutic agents.

Pseudomonas aeruginosa is an opportunistic pathogen that infects patients suffering from low immune activity and exhibits resistance to a broad spectrum of antibiotics. Multiantibiotic resistance in this organism is largely attributable to low outer membrane permeability and expression of multidrug efflux pumps or transporters (*4*, *6*). Although a number of multidrug efflux pumps have been reported in *P. aeruginosa* to date (*7*−*9*), the MexA-MexB-OprM pump is constitutively expressed in the wild-type strains, thus contributing to the intrinsic antibiotic resistance of this organism (*10*−*12*). Upon mutation of the *mexR* regulatory gene or classically the *nalB* gene, the cells overexpress MexA-MexB-OprM and gain a higher level of multiantibiotic resistance than the wild-type strains (*13*−*16*).

The MexA-MexB-OprM efflux pump consists of tripatile subunits including the polytopic drug-proton antiporter MexB, the inner membrane anchored periplasmic lipoprotein MexA, and the outer membrane-associated lipoprotein OprM (*11*). The MexB subunit belonging to the resistance-nodulation-division (RND)[1] super-family consists of 1046 amino acid residues and traverses the inner membrane 12 times (*1*, *17*, *18*). The protein has two large periplasmic domains in the transmembrane segments, TMS-1/2 and TMS-7/8 (a loop connecting the TMSs is expressed throughout this paper as loop-1/2 for a loop connecting TMS-1 and -2), consisting of 311 and 314 amino acid residues, respectively (*17*). All these predicted structures have been confirmed by X-ray crystallographic analysis of AcrB, an *Escherichia coli* analogue of MexB (*19*). MexA subunit and its family proteins, designated as the membrane fusion proteins, were assumed to bypass the periplasmic space bridging the inner and outer membranes (*3*, *20*, *21*). The OprM subunit and its family outer membrane proteins were assumed to form the xenobiotic exit-channel across the outer membrane (*3*, *6*, *22*, *23*). However, a mechanism has not yet been proposed to explain how the fatty acid-modified OprM is able to form a transmembrane channel.

Most RND super-family proteins in prokaryotes bear 12 TMSs and tandem repeats (*18*). In fact, the amino acid sequence of the amino-proximal half of MexB showed a high similarity to the carboxyl-proximal half, forming a mirror

† This study was supported by grants from the Ministry of Education, Culture, Sport, Science and Technology, Japan Society for Promotion of Science, the Ministry of Health, Labor and Welfare, Tokai University Research Project, and Tokai University School of Medicine Research Project. S.E. is a recipient of the Tokai University School of Medicine Research Fellowship.

* Corresponding author. Tel.: 81-463-93-5436. Fax: 81-463-93-5437. E-mail: nakae@is.icc.u-tokai.ac.jp.

[1] Abbreviations: RND, resistance nodulation cell division; TMS, transmembrane segment; SDS−PAGE, sodium dodecyl sulfate polyacrylamide gel electrophoresis; LB, Luria−Bertani medium; MIC, minimum growth inhibitory concentration (of antibiotic); OG, *n*-octyl-*β*-D-glucopyranoside; IPTG, isopropyl-*β*-D-thiogalactopyranoside.

10.1021/bi0300074 CCC: $25.00
Published on Web 05/21/2003

Table 1: Bacterial Strains and Plasmids Used

strains or plasmids	description	source or ref
	P. aeruginosa strains	
PAO4290	*leu-10, argF10, aph-9004*; FP^-	H. Matsumoto (*12*)
TNP071	Δ*mexB*; derivative of PAO4290	H. Yoneyama (*12*)
TNP073	Δ*mexA* Δ*mexB*; derivative of PAO4290	H. Yoneyama (*12*)
TNP076	Δ*mexA* Δ*mexB* Δ*oprM*; derivative of PAO4290	H. Yoneyama (*12*)
	Plasmids	
pMMB67EH	broad-host range vector; Amp^r, IncQ	J. P. Fürste (*46*)
pMEXB1	pMMB67EH derivative carrying *mexB* gene	H. Yoneyama (*12*)
pBSK-mexB	pBluescript SK(−) carrying a 3.9-kb *Sal*I fragment of pMEXB1	L. Guan (*31*)
pMMB-B-his	pMMB67EH derivative carrying histidine-tagged-*mexB*	this paper
pMBS510	pMMB-B-his derivative carrying the severed *mexB* (1−510 or 511−1046)	this paper
pMNH	pMBS510 derivative carrying the 5′ portion of *mexB*	this paper
pMCH511	pMMB-B-his derivative carrying the 3′ portion of *mexB*	this paper
pMCH-K939A	pMCH511 derivative containing K939A mutation	this paper

image, which is a phenomenon that is probably attributable to intragenic tandem duplication (*1*, *17*, *18*). Some of the exceptional cases are as follows. The SecDF family proteins in many bacteria (subfamily of RND super family) involved in protein translocation are expressed as two distinct polypeptide chains (*18*). SecD and SecF, each bearing six TMSs, form a complex in the membrane (*24*−*27*). In contrast, SecDF in *Bacillus subtilis* was produced as a large single polypeptide chain containing 12 putative TMSs (*28*). On one hand, the archaeal RND-family homologue protein, ORF MJ1562, in *Methanococcus jannaschii* has six TMSs and does not show any internal duplication (*18*, *29*). It was postulated that this protein is likely to function by forming a homodimer bearing 12 TMSs (*18*). Accordingly, it is likely that the RND family proteins containing an internal duplication can function by means of a half molecule. More recently, we have reported a possibility that the RND-transporters can expel xenobiotics directly from periplasm without crossing the cytoplasmic membrane (*30*).

Since the MexB protein has internal tandem repeats much like other RND family proteins, it is conceivable that either half-size MexB is functional. Alternatively, the protein divided into two halves could be functional when the two halves are coexpressed, as we proposed that TMS-4 and -10 in amino and carboxyl proximal halves, respectively, are in close proximity (*31*, *32*). Thus, we divided the *mexB* gene into two halves and expressed them either separately or in combination. The cells that expressed both amino- and carboxyl-proximal half fragments simultaneously showed restored antibiotic resistance, and these polypeptides were found in an aggregate. In contrast, cells that expressed only the amino- or the carboxyl-proximal half appeared to be dysfunctional. These results suggested that the formation of a complex of the amino- and carboxyl-proximal halves of MexB might be essential for transport activity.

MATERIALS AND METHODS

Bacterial Strains and Plasmids. Bacterial strains and plasmids used in this study are listed in Table 1.

Construction of Plasmids. The MexB protein containing six extra histidine residues at the carboxyl terminal end was constructed in plasmid pMEXB1 by adding the codons for six histidines. The 3′ region of *mexB* was amplified by PCR using the primers P1-mexB (5′- CAAGCAATTGCCGAAAGGCG-3′) and 6xhis (5′-CGACGTCGACCGTTTCATATCAgtgatggtgatggtgatgTTGCCCCTTTTCGACGGACGCCTG-3′. (The *Sal*I site, the stop codon, and the six histidine codons are indicated by an underline, a double underline, and in lowercase, respectively.) Purified PCR product was treated with *Mun*I and *Sal*I and ligated to the *Mun*I- and *Xho*I-treated pBSK-mexB. The resultant plasmid pBSK-B-his was then digested with *Apa*I. The linearized plasmid was treated with T4 DNA polymerase and ligated with *Hin*dIII linker (New England BioLabs) yielding pBSK-BhisH. A 0.9-kb *Mun*I-*Hin*dIII fragment containing the 3′ region of the *mexB* gene with six histidine codons was replaced in the parent plasmid pMEXB1.

To express both the amino- and the carboxyl-proximal halves of MexB simultaneously, pMBS510 carrying the two halves of *mexB* was constructed as follows. A DNA sequence of 21 nucleotides (5′-TGATC*AAGGGGA*TTCCATATG-3′) containing a stop codon (underline), a Shine-Dalgarno (italics), and an initiation codon (double underline) was inserted between the 1530th and 1531st nucleotide sequences of *mexB* by the overlapped extension PCR method (*33*). Briefly, two pairs of primers (the first set: MBS-510U, 5′-CATATGGAATCCCCTTGATCAGCCCTTGTGCTCGCCATGGTCG-3′ and P15-mexB, 5′-ACCATCATCGGCAAGACCC-3′, and the second set: MBS-510D, 5′-TGATCAAGGGGATTCCATATGGGCTTCTTCGGCTGGTTCAAC-3′ and P4-mexB, 5′-TTCGATGGCCGCCTCGACGATG-3′) were used. Two fragments of PCR products were used for overlap extension PCR with a pair of primers, P15-mexB and P4-mexB. The resulting product corresponding to the 697th through 2892nd nucleotides of *mexB* with a 21-nucleotide insert at the middle was digested with *Bsi*WI and *Mun*I and subsequently used to replace the corresponding fragment within the parent plasmid pMMB-B-his (Figure 1).

The plasmid pMCH511containing the 3′ half of *mexB* was constructed by the overlap PCR method (*33*). In the first PCR reaction, two pairs of primers (first set: RVM, 5′-GAGCGGATAACAATTTCACACAGG-3′ and CH2-510U, 5′-GTTGAACCAGCCGAAGAAGCCCATTACGAATCCCCTTGATCA-3′ and the second set: CH2-510D, 5′-TGATCAAGGGGATTCGTAATGGGCTTCTTCGGCTGGTTCAAC-3′ and R-pMMB67EH, 5′-CTCTCATCCGCCAAAACAGC-3′) were used with a pMEXB1 as a template. The second PCR reaction was carried out using a pair of primers, RVM and R-pMMB67EH. The product

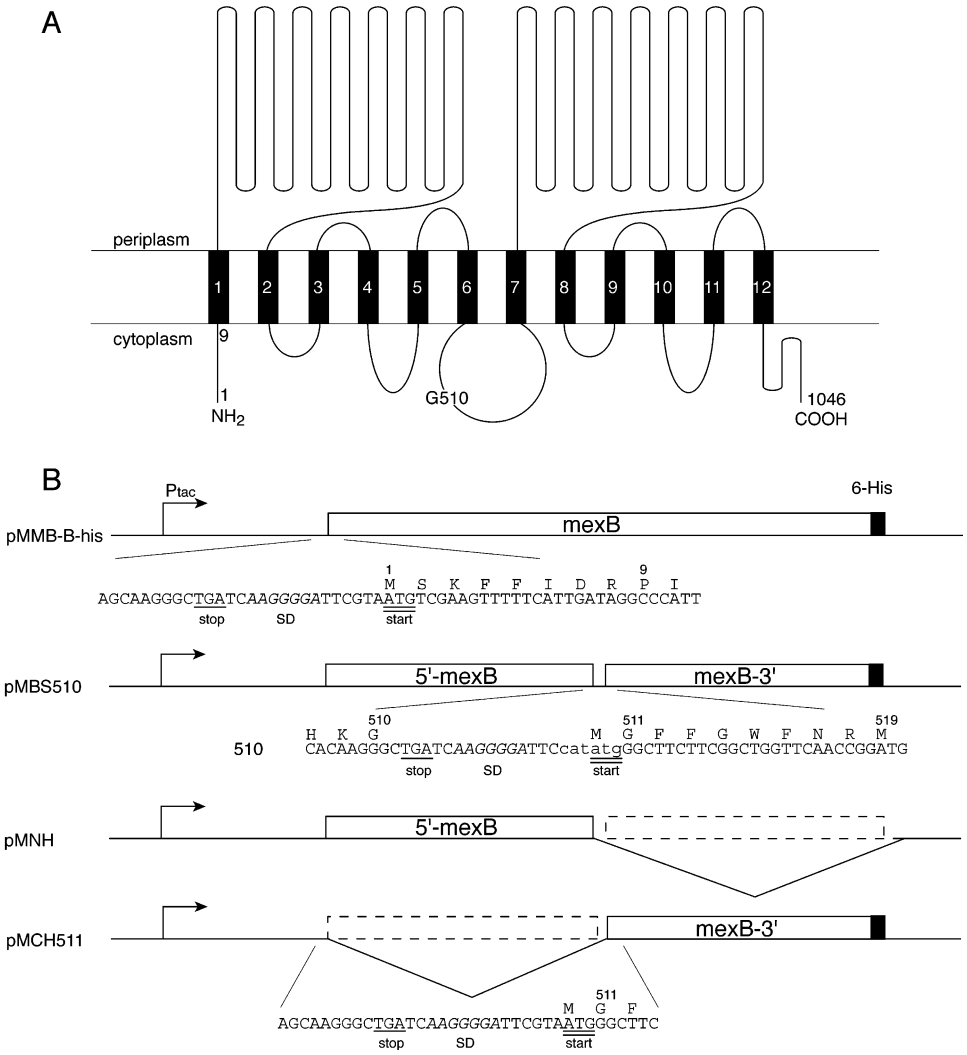

FIGURE 1: Schematic representation of the two-dimensional structure of MexB and construction of plasmids carrying the half-size *mexB*. (A) The membrane topology and the extramembrane loops were drawn on the basis of results reported previously (*17*). The protein was divided at G510. (B) Schematic representation of construction of the plasmid coding for amino- or carboxyl-proximal halves of *mexB*. For details, see Materials and Methods.

of the second PCR reaction was digested with *Eco*RI and *Mun*I. This procedure deleted the amino-proximal half of *mexB*, and the remaining carboxyl-proximal half of the fragment was inserted in the parent plasmid, pMMB-B-his.

To express the carboxyl-proximal half of MexB containing Ala as a substitute for Lys939, a site-directed mutation was introduced into the 3′ half of *mexB* gene carried by pMCH511. Mutagenesis was carried out using the QuikChange site-directed mutagenesis kit (Stratagene) and primers K939A-s (5′-CCATCGGCCTGTCGGCGGCGAACGCCATTCTCATCG-3′) and K939A-a (5′-CGATGAGAATGGCGTTCGCCGCCGACAGGCCGATGG-3′).

The fragment encoding the amino-proximal half of MexB was constructed as follows. The plasmid pMBS510 was digested with *Nde*I and *Hin*dIII, and the large *Nde*I-*Hin*dIII fragment was treated with T4 DNA polymerase and then self-ligated to yield pMNH. All the PCR reactions were carried out with high-fidelity *Pfu Turbo* DNA polymerase (Stratagene). The nucleotide sequence of all constructs was confirmed.

Preparation of Polyclonal Antisera Specific to MexY. To obtain antibody specific to MexY, oligopeptides with the following sequence KIVESRLPESVRRDGIYVEK, RRVEGVGKVETWGAEYAMRI, QGEAPQIRLDIDRRKAETLG, and QADRRKRLGIDDIGRLHVRN were synthesized. Rabbit antibody was raised against a mixture of these oligopeptides by SAWADY Technology Co., Ltd. (Tokyo, Japan).

Assessment of MexB Function by Determination of the Minimum Growth Inhibitory Concentration (MIC) of Antibiotics. Since the transport assay in the mutant MexB was technically difficult, we determined the MICs of antibiotics to access the transporter activity by a 2-fold agar dilution method using Mueller-Hinton II agar (Becton Dickinson Microbiology Systems) in the presence of 2 mM isopropyl-β-D-thiogalactopyranoside (IPTG). The plates were incubated at 37 °C for 18 h or 28 °C for 22 h.

Isolation of Crude Membrane Fraction, Sodium Dodecyl Sulfate−Polyacrylamide Gel Electrophoresis (SDS−PAGE) and Immunoblot Assay. Cells were grown in 20 mL of LB medium containing 100 μg/mL of sulbenicillin at 37 °C to $A_{600} = 0.6$. Next, 2 mM IPTG was added, and the cells were harvested by centrifugation after incubating for an additional 2 h. To express protein at a low temperature, the culture temperature was reduced to 28 °C immediately after adding

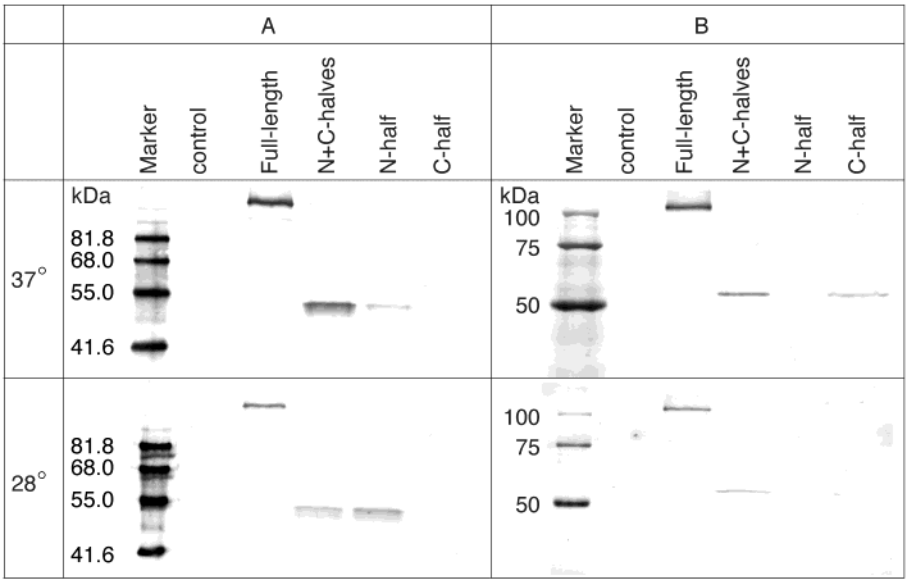

FIGURE 2: Expression of MexB divided into two-halves membrane fractions were prepared from TNP071 harboring the appropriate plasmid and lacking MexB. The envelope fraction containing 10 μg of protein was subjected to 10% SDS−PAGE except that 100 μg of the C-half was applied. (A) The amino proximal half of MexB was visualized with anti-MexB antibody. (B) The carboxyl-proximal half of MexB was stained with anti-penta-his antibody. Abbreviations: control, vector (pMMB67EH); full-length, histidine-tagged full-length MexB (pMMB-B-his); N+C-halves, both amino- and carboxyl-half (pMBS510); N-half, amino-proximal half (pMNH); C-half, carboxyl-proximal half (pMCH511). Reference protein markers are indicated in kiloDaltons.

2 mM IPTG and was then incubated for an additional 5 h. The total membrane fraction was prepared as described elsewhere (*34*). SDS−PAGE was carried out as described previously (*35*). The MexB protein was visualized by immunoblot assay using rabbit polyclonal antisera against MexB (a loop-1/2) (*12*) or by Penta-His Antibody (Qiagen).

Nickel-Chelate Chromatography. Cells were grown in 20 mL of LB medium supplemented with 100 μg/mL of sulbenicillin at 37 °C until A_{600} reached 0.6. Incubation temperature was shifted to 28 °C immediately after adding 2 mM IPTG and incubated for an additional 5-h period. Cells were harvested, and the total membrane fraction was prepared as described above. Crude membrane fraction was suspended in 400 μL of the binding buffer containing 50 mM sodium phosphate, pH 7.5, 100 mM NaCl, 10 mM imidazole, and 2% *n*-octyl-β-D-glucopyranoside (OG), and the mixture was incubated for 30 min on ice. The mixture was centrifuged at 100,000*g* for 20 min, and supernatant was loaded onto a nickel-nitrilotriacetic acid (Ni-NTA) spin column (Qiagen) equilibrated with the binding buffer. The column was washed five times with 400 μL of the wash buffer containing 50 mM sodium phosphate, pH 7.5, 100 mM NaCl, 20 mM imidazole, and 2% OG and was then eluted with 400 μL of the elution buffer containing 50 mM sodium phosphate, pH 7.5, 100 mM NaCl, 500 mM imidazole, and 2% OG.

RESULTS

Construction and Expression of the mexB Gene Encoding a Half Molecule of MexB. The MexB molecules showed internal tandem repeats at the amino- and the carboxyl-proximal halves with an amino acid identity of about 30% (Figure 1). To divide the MexB molecule into two halves, it was essential to confirm that modification of cytoplasmic loop-6/7 did not interfere with the pump function. We confirmed that insertion of a linker containing 24 amino acid residues derived from the tobacco-etch-virus (TEV) protease-susceptible peptide (*36*) at His508 did not interfere with the pump function (data not shown). Thus, the MexB peptide was divided at Gly510 or Gly511 as described in Materials and Methods.

To facilitate purification and subsequent protein analysis, a hexa-histidine-tag was attached to the carboxyl-terminal end of the carboxyl-proximal half of MexB, and the proteins were expressed in cells lacking MexB. When both the amino- and the carboxyl-proximal halves of the molecules were coexpressed from the separate open reading frames, we found both fragments with the expected molecular masses of 54 and 59 kDa, respectively. When proteins were visualized by the anti-MexB (loop-1/2) antibody, the amount of protein appeared comparable with that of the full-length MexB (Figure 2A). As the same materials were stained with anti-His antibody (carboxyl end), we observed a less amount of protein than in the full-length MexB, thereby suggesting that the carboxyl-proximal half was more labile than the amino-proximal half (Figure 2B). The amino-proximal half molecule expressed alone appeared faint at 37 °C, although it was fully expressed at 28 °C (Figure 2A). The carboxyl-proximal half molecules expressed without amino-proximal counterpart appeared faint at 37 °C even if a 5-fold greater quantity of the protein was loaded, and expression was even fainter at 28 °C (Figure 2B).

Function of the MexB Protein Divided into Two Halves. We have established a method to assess the function of the xenotiotic transporter by monitoring real-time accumulation of fluorescent dye, and the results obtained from this method correlated well with the MIC values of antibiotics without exception (*31*, *32*, *37*−*39*). Since cells expressing mutant MexB tend to aggregate making it difficult to obtain a homogeneous cell suspension, we monitored the MexB function by determining the MICs of antibiotics in the cells that expressed MexB. The cell-free or liposome transport assay method is not available yet for the three-component

Table 2: Antimicrobial Susceptibility of Cells Expressing a Half-Size MexB

strain	MexB derivative	MIC (μg/mL) of[a]			
		aztreonam	nalidixic acid	novobiocin	chloramphenicol
		37 °C			
PAO4290	wild-type	3.13	200	1600	100
TNP071	Δ*mexB*	0.2	25	50	6.25 ∼ 12.5
TNP071/pMMB67EH		0.2	25	50	6.25 ∼ 12.5
TNP071/pMEXB1	wild-type	3.13	100	400 ∼ 800	25 ∼ 50
TNP071/pMMB-B-his	histidine-tagged MexB	3.13	100	400 ∼ 800	25 ∼ 50
TNP071/pMBS510	N-half (1−510) + C-half (511−1046)	3.13	100	200 ∼ 400	12.5
TNP071/pMNH	N-half (1−510)	ND[b]	ND	ND	ND
TNP071/pMCH511	C-half (511−1046)	0.39	12.5	50	6.25
TNP071/pMCH-K939A	C-half (511−1046), K939A mutation	0.39	12.5	50	6.25
		28 °C			
PAO4290	wild-type	3.13	50	400	25
TNP071	Δ*mexB*	0.2	6.25	25 ∼ 50	3.13
TNP071/pMMB67EH		0.2	6.25	50	3.13
TNP071/pMEXB1	wild-type	3.13	25 ∼ 50	200	25
TNP071/pMMB-B-his	histidine-tagged MexB	3.13	25 ∼ 50	200	25
TNP071/pMBS510	N-half (1−510) + C-half (511−1046)	3.13	12.5	200	25
TNP071/pMNH	N-half (1−510)	0.2 ∼ 0.39	6.25	12.5	3.13
TNP071/pMCH511	C-half (511−1046)	0.39	6.25	<12.5	3.13
TNP071/ pMCH-K939A	C-half (511−1046), K939A mutation	0.39	6.25	<12.5	3.13

[a] The MICs shown are representative of several repeated experiments. [b] ND, not determined.

RND-xenobiotic transporter.

The MICs of aztreonam, nalidixic acid, novobiocin, and chloramphenicol in cells expressing both the amino and the carboxyl halves of MexB were 3.13, 100, 200−400, and 12.5 μg/mL, respectively, which is comparable with the MICs in the cells producing the full-length MexB at 37 °C (Table 2). The same results were confirmed at 28 °C. These results established that the MexB protein divided at the middle retained its pump function when both halves were expressed together.

As the amino-proximal half of MexB only was expressed at 37 °C, the cells showed poor growth. On the other hand, the same cells showed that the MIC of aztreonam was 0.2−0.39 μg/mL at 28 °C, which was nearly comparable with that in cells lacking MexB. Cells producing the carboxyl-proximal half of MexB showed only a 2-fold higher MIC of aztreonam than that in cells lacking MexB, which was 8-fold lower than in the cells producing the wild-type MexB. The possibility cannot be ruled out, therefore, that the carboxyl-proximal half of the protein has a low level of transport activity. To clarify this ambiguity, we introduced the Lys939Ala mutation into the carboxyl-proximal half of MexB, which is known to knock out the pump function (*31*). Cells expressing this mutant MexB showed an MIC of aztreonam identical to that of cells expressing the carboxyl-proximal half of MexB only (Table 2). Therefore, we concluded that the half-size MexB alone failed to transport xenobiotics.

Interaction of the Amino- and Carboxyl-Proximal Halves of MexB. Since the two-half-size MexBs expressed together appeared to be functional, it is conceivable that the functional MexB requires the interaction of both amino- and carboxyl-proximal fragments. To test this possibility, we expressed both amino- and carboxyl-proximal halves of MexBs simultaneously. The extracts were subjected to nickel-chelate column chromatography to trap the carboxyl-half fragment, and the proteins were visualized with antibodies against a loop-1/2 (for an amino-half) and penta-histidine (for a carboxyl-half). If the amino- and carboxyl-halves of molecules form an aggregate, it would be expected that the nonhistidine-tagged amino-half MexB molecules would be coeluted in the fraction containing the histidine-tagged carboxyl-half MexB. When the nickel-column eluates were stained with the anti-His antibody, the materials purified from the cells bearing both amino- and carboxyl-proximal-His halves showed a prominent protein band corresponding to the expected molecular mass (Figure 3A, right panel, second row, lane E). On one hand, cells only producing the amino-proximal MexB did not show a detectable protein band because of lack of the histidine-tag (Figure 3A, right panel, first row, lane E).

Interestingly, the nickel-column eluates from cells producing both the amino- and the carboxyl-proximal halves of MexB showed a prominent protein band reactive with the anti-amino-proximal half antibody and a size corresponding to the amino-proximal MexB (Figure 3A, left panel, second row, lane E), suggesting that this fragment formed a surfactant-resistant aggregate with the carboxyl-proximal MexB. This result was interpreted to mean that amino- and carboxyl-proximal fragments were the subunits in the reconstituted MexB.

One may argue that this result may have been a consequence of subunit interaction via the surfactant micelle. To answer this question, we constructed the amino-proximal MexB tagged with T7-epitope or hexahistidine and coexpressed. Unfortunately, both of these proteins were not produced to a level that could be detected with antibody. Next, we examined whether the MexY protein, which is a homologue of MexB and is supposed to not interact with MexB (*7*), could be copurified with carboxyl-proximal halves of MexB. MexY was induced in the presence of subinhibitory

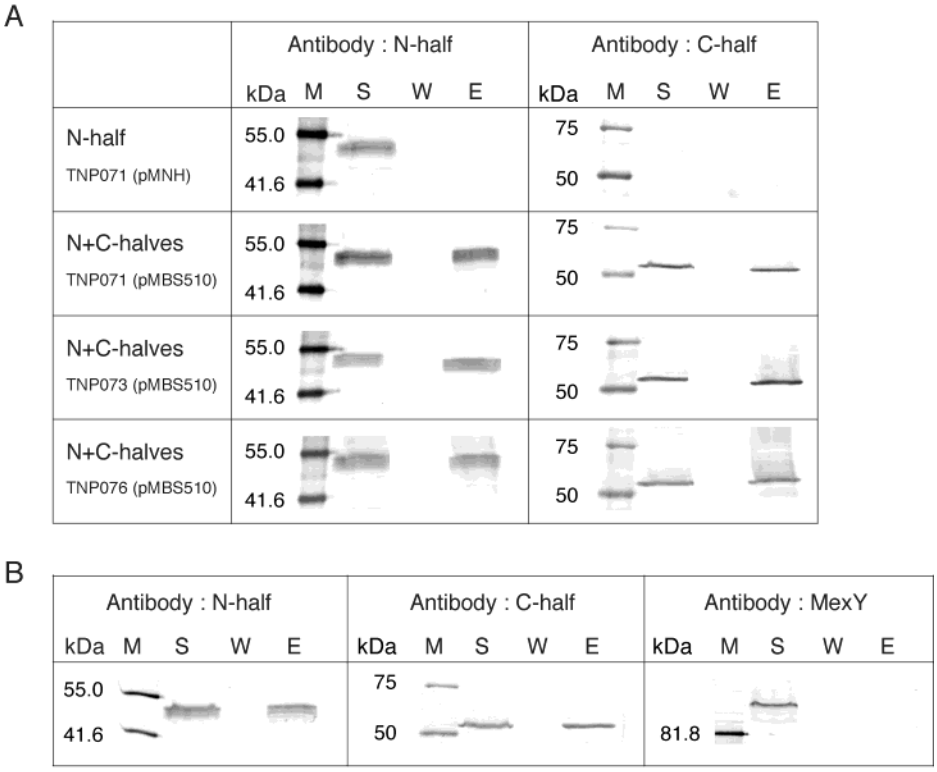

FIGURE 3: Immunoblot analysis of half-molecules of MexB isolated by nickel-chelate chromatography. (A) Co-purification of amino-proximal half of MexB with carboxyl-proximal half of MexB. The crude membrane fraction was prepared from *P. aeruginosa* cells harboring the respective plasmid, solubilized with 2% of OG and subjected to nickel-chelate chromatography as described under Materials and Methods. Equivalent volumes of samples were subjected to SDS−PAGE. Amino- and carboxyl-proximal half of MexB were visualized with anti-MexB antibody and anti-penta-his antibody, respectively. Abbreviations: N-half, amino-proximal half; N+C-halves, both amino- and carboxyl-proximal halves; M, molecular weight marker; S, crude envelope fraction; W, column wash with 20 mM imidazole buffer; E, column eluate with 500 mM imidazole buffer. Strains TNP071, TNP073, and TNP076 lack *mexB*, *mexA*, and *mexB* and *mexA*, *mexB*, and *oprM*, respectively. The plasmid is shown in parentheses. (B) Experiments to test possible interaction of MexY with carboxyl-proximal half of MexB. The crude membrane fraction was prepared from *P. aeruginosa* TNP071 carrying pMBS510 as described above except that the cells were cultured in the presence of 100 μg/mL tetracycline. MexY was visualized with anti-MexY antibody.

concentration of tetracycline (Figure 3B, right panel, lane S). In contrast to the amino-proximal halves of MexB (Figure 3B, left panel, lane E), no detectable MexY was recovered from a carboxyl-half-MexB column (Figure 3B, right panel, lane E). Therefore, copurification of the amino-proximal MexB with the carboxyl-proximal MexB was not a consequence of cosolubilization of both halves in detergent micelles.

Since the MexB protein requires the presence of MexA and OprM for the pump function, it is conceivable that the complex was formed with the mediation of MexA and OprM. To test this possibility, amino- and carboxyl-halves of MexB were expressed in cells lacking *mexA*/*mexB* or *mexA*/*mexB*/*oprM*. The results depicted in Figure 3A (left panel, rows 3 and 4, lane E) showed that the amino-proximal half of MexB was clearly recovered from the cells lacking either MexA or OprM. These results indicated that the amino-half fragment directly interacts with the carboxyl-half fragment independently of the presence or absence of MexA and OprM.

One may also argue that MexA and OprM were not associated with MexB. This view is unlikely to be valid at least for MexA since MexA could be copurified with MexB (data not shown). However, there is no firm evidence available at present that the OprM subunit forms a tight complex with MexB or the MexA−MexB complex.

DISCUSSION

We have reported in this paper that expression of the amino- or carboxyl-proximal half of MexB produced a half-size MexB. However, these truncated proteins were totally inactive as xenobiotic transporters. Although substrate-binding site(s) of an RND-type multidrug transporter has not been identified, Mao et al. have reported that the mutations that altered substrate specificity of MexD, a MexB homologue, were distributed in both halves (*40*). More recently, we showed that the RND-type transporters of *P. aeruginosa* select substrates by the two large periplasmic domains as demonstrated by the experiment that the mosaic protein bearing two large periplasmic domains of MexB and the rest from MexY selected the substrates for MexB but not for MexY (*30*). Furthermore, the hybrid proteins bearing only one large periplasmic domain of MexB and the rest from MexY recognized neither MexB nor MexY substrate. Thus, it is less likely that the RND transporters select substrates by only one-half of the protein. Since the bacterial RND transporters function in collaboration with the periplasmic and outer membrane components, another possible explanation could be that one-half molecules of MexB alone failed to interact with these subunits.

This paper reported that expression of the amino- and carboxyl-proximal halves of MexB from the independent open reading frames yielded a functional MexB protein

consisting of two different polypeptides. In fact, we have demonstrated that the amino-proximal half could be copurified with the carboxyl-proximal half suggesting that both of these two divided molecules were part of the functional assembly. Our recent report supported this conclusion that TMS-4 and -10 are in close contact via a salt bridge, which is likely to form the proton pathway necessary to energize the transporter (*31*, *32*). This assumption was also strongly supported by the fact that the crystallographic structure of AcrB showed both inter- and intramolecular interactions, the long arm of the MexB periplasmic domain extended profoundly into the neighboring subunit of the AcrB trimer (*19*), and both periplasmic loops and TMSs of the same polypeptide closely interacted. To the best of our knowledge, this is the first demonstration in prokaryote xenobiotic transporters of the restoration of transporter activity from two separate amino- and carboxyl-halves of fragments.

One may argue that MexB protein reconstituted from two half fragments might be less active than the chromosomally encoded full-length MexB because the cells producing a large amount of the reconstituted proteins showed comparable MICs to that of the wild-type cells. However, this view seems less likely since the MICs of antibiotics in cells producing plasmid-borne full-length MexB appeared comparable to that in the wild-type cells (Table 2). A likely possibility would be that cells expressing the plasmid borne MexB might not have the full amount of the MexA and OprM subunits. In fact, the *mexR* mutant expressing derepressed levels of MexA, MexB, and OprM exhibits severalfold higher MICs of antibiotics than cells expressing plasmid-borne MexB (*16*, *41*).

Eukaryotic transporters with internal tandem repeats, such as P-glycoprotein (MDR1), multi-drug resistance-related protein (MRP), and yeast **a**-factor transporter (STE6), were reported to form a functional protein unit when the amino- and carboxyl-halves of the proteins were coexpressed (*42*−*45*). These transporters expressing either the amino- or the carboxyl-proximal half molecule failed to show transporter activity. These observations were consistent with the data presented in this paper.

REFERENCES

1. Paulsen, I. T., Brown, M. H., and Skurray, R. A. (1996) *Microbiol. Rev. 60*, 575−608.
2. Saier M. H, Jr., Paulsen, I. T., Sliwinski, M. K., Pao, S. S., Skurray, R. A., and Nikaido, H. (1998) *FASEB J. 12*, 265−274.
3. Ma, D., Cook, D. N., Hearst, J. E., and Nikaido, H. (1994) *Trends Microbiol. 2*, 489−493.
4. Nakae, T., Yoshihara, E., and Yoneyama, H. (1997) *J. Infect. Chemother. 3*, 173−183.
5. Nikaido, H. (1998) *Curr. Opin. Microbiol. 1*, 516−523.
6. Nikaido, H. (1994) *Science 264*, 382−388.
7. Poole, K. (2001) *J. Mol. Microbiol. Biotechnol. 3*, 255−264.
8. Chuanchuen, R., Narasaki, C. T., and Schweizer, H. P. (2002) *J. Bacteriol. 184*, 5036−5044.
9. Aendekerk, S., Ghysels, B., Cornelis, P., and Baysse, C. (2002) *Microbiology 148*, 2371−2381.
10. Morshed, S. R., Lei, Y., Yoneyama, H., and Nakae, T. (1995) *Biochem. Biophys. Res. Commun. 210*, 356−362.
11. Poole, K., Krebes, K., McNally, C., and Neshat, S. (1993) *J. Bacteriol. 175*, 7363−7372.
12. Yoneyama, H., Ocaktan, A., Tsuda, M., and Nakae, T. (1997) *Biochem. Biophys. Res. Commun. 233*, 611−618.
13. Masuda, N., Sakagawa, E., Ohya, S., Gotoh, N., Tsujimoto, H., and Nishino, T. (2000) *Antimicrob. Agents Chemother. 44*, 2242−2246.
14. Poole, K., Tetro, K., Zhao, Q., Neshat, S., Heinrichs, D. E., and Bianco, N. (1996) *Antimicrob. Agents Chemother. 40*, 2021−2028.
15. Rella, M., and Haas, D. (1982) *Antimicrob. Agents Chemother. 22*, 242−249.
16. Saito, K., Yoneyama, H., and Nakae, T. (1999) *FEMS Microbiol. Lett. 179*, 67−72.
17. Guan, L., Ehrmann, M., Yoneyama, H., and Nakae, T. (1999) *J. Biol. Chem. 274*, 10517−10522.
18. Tseng, T. T., Gatwick, K. S., Kollman, J., Park, D., Nies, D. H., Goffeau, A., and Saier, M. H, Jr. (1999) *J. Mol. Microbiol. Biotechnol. 1*, 101−125.
19. Murakami, S., Nakashima, R., Yamashita, E., and Yamaguchi, A. (2002) *Nature 419*, 587−593.
20. Yoneyama, H., Maseda, H., Kamiguchi, H., and Nakae, T. (2000) *J. Biol. Chem. 275*, 4628−4634.
21. Saier, M. H., Jr., Tam, R., Reizer, A., and Reizer, J. (1994) *Mol. Microbiol. 11*, 841−847.
22. Nakae, T. (1995) *Microbiol. Immunol. 39*, 221−229.
23. Nakajima, A., Sugimoto, Y., Yoneyama, H., and Nakae, T. (2000) *J. Biol. Chem. 275*, 30064−30068.
24. Pogliano, K. J., and Beckwith, J. (1994) *J. Bacteriol. 176*, 804−814.
25. Gardel, C., Johnson, K., Jacq, A., and Beckwith, J. (1990) *EMBO J. 9*, 3209−3216.
26. Economou, A. (1998) *Mol. Microbiol. 27*, 511−518.
27. Duong, F., and Wickner, W. (1997) *EMBO J. 16*, 2756−2768.
28. Bolhuis, A., Broekhuizen, C. P., Sorokin, A., van Roosmalen, M. L., Venema, G., Bron, S., Quax, W. J., and van Dijl, J. M. (1998) *J. Biol. Chem. 273*, 21217−21224.
29. Bult, C. J., White, O., Olsen, G. J., Zhou, L., Fleischmann, R. D., Sutton, G. G., Blake, J. A., Fitzgerald, L. M., Clayton, R. A., Gocayne, J. D., Kerlavage, A. R., Dougherty, B. A., Tomb, J. F., Adams, M. D., Reich, C. I., Overbeek, R., Kirkness, E. F., Weinstock, K. G., Merrick, J. M., Glodek, A., Scott, J. L., Geoghagen, N. S., and Venter, J. C. (1996) *Science 273*, 1058−1073.
30. Eda, S., Maseda, H., and Nakae, T. (2003) *J. Biol. Chem. 278*, 2085−2088.
31. Guan, L., and Nakae, T. (2001) *J. Bacteriol. 185*, 1734−1739.
32. Yoneyama, H., Maseda, H., Yamabayashi T., Izumi, S., and Nakae, T. (2002) *Biochem. Biophys. Res. Commun. 292*, 513−518.
33. Ho, S. N., Hunt, H. D., Horton, R. M., Pullen, J. K., and Pease, L. R. (1989) *Gene 77*, 51−59.
34. Gotoh, N., Tsujimoto, H., Tsuda, M., Okamoto, K., Nomura, A., Wada, T., Nakahashi, M., and Nishino, T. (1998) *Antimicrob. Agents Chemother. 42*, 1938−1943.
35. Laemmli, U. K. (1970) *Nature 227*, 680−685.
36. Ehrmann, M., Bolek, P., Mondigler, M., Boyd, D., and Lange, R. (1997) *Proc. Natl. Acad. Sci. U.S.A. 94*, 13111−13115.
37. Germ, M., Yoshihara, E., Yoneyama, H., and Nakae, T. (1999) *Biochem. Biophys. Res. Commun. 261*, 452−455.
38. Ocaktan, A., Yoneyama, H., and Nakae, T. (1997) *J. Biol. Chem. 272*, 21964−21969.
39. Yoneyama, H., Ocaktan, A., Gotoh, N., Nishino, T., and Nakae, T. (1998) *Biochem. Biophys. Res. Commun. 244*, 898−902.
40. Mao, W., Warren, M. S., Black, D. S., Satou, T., Murata, T., Nishino, T., Gotoh, N., and Lomovskaya, O. (2002) *Mol. Microbiol. 46*, 889−901.
41. Yoneyama, H., Ocaktan, A., Gotoh, N., Nishino, T., and Nakae, T. (1998) *Biochem. Biophys. Res. Commun. 244*, 898−902.
42. Loo, T. W., and Clarke, D. M. (1994) *J. Biol. Chem. 269*, 7750−7755.
43. Loo, T. W., and Clarke, D. M. (1996) *J. Biol. Chem. 271*, 27488−27492.
44. Gao, M., Loe, D. W., Grant, C. E., Cole, S. P., and Deeley, R. G. (1996) *J. Biol. Chem. 271*, 27782−27787.
45. Berkower, C., and Michaelis, S. (1991) *EMBO J. 10*, 3777−3785.
46. Furste, J. P., Pansegrau, W., Frank, R., Blocker, H., Scholz, P., Bagdasarian, M., and Lanka, E. (1986) *Gene 48*, 119−131.

BI0300074